ELSEVIER

Nuclear Instruments and Methods in Physics Research B 151 (1999) 29–41

NIM B
Beam Interactions with Materials & Atoms

www.elsevier.nl/locate/nimb

Ion-beam modification of polymeric materials – fundamental principles and applications

Eal H. Lee [1]

Metals and Ceramics Division, Oak Ridge National Laboratory, P.O. Box 2008, Oak Ridge, TN 37831-6376, USA

Abstract

When an energetic ion traverses a polymer medium, it loses its energy by electronic and nuclear processes. In the past, considerable research efforts have been devoted to understand the effects of the electronic and nuclear processes in materials. There have been, however, some conflicting reports regarding the roles of electronic and nuclear stopping in producing property changes in polymeric materials, namely the magnitude of cross-linking and scission. A consensus derived from the work conducted at ORNL indicates that electronic stopping is largely responsible for cross-linking and nuclear stopping for scission, although both processes can cause cross-linking as well as scission. The most important parameter for cross-linking is found to be the energy deposited per unit ion path length or linear energy transfer (LET). The mechanisms involved with property changes are discussed by clarifying the concepts of nuclear and electronic stopping, LET, tracks, and spurs. Experimental evidence to support the views are presented. Also addressed are specific property changes induced by ion-beams, which may be of use for industrial applications. © 1999 Elsevier Science B.V. All rights reserved.

PACS: 61.80.-x; 82.50.Gw; 78.65.He
Keywords: Ion-beam; LET effects; Cross-linking; Scission; Tracks; Spurs; Hardness

1. Introduction

In the past, radiation effects have been the subject of intense investigation in radiation chemistry, mainly to understand the radiolysis and polymerization mechanisms induced by ionizing radiation such as e-beam and γ-rays. However, work at ORNL showed that materials' response to high energy ion-beams was considerably different from those induced by e-beam and γ-rays. In that work, it was well established that cross-linking or scission efficiency depends not only upon polymer structure but also upon the characteristics of the radiation sources, namely ion energy and ion species [1]. For example, poly(methyl methacrylate) (PMMA) degraded and became more soluble in solvents when subjected to e-beam or γ-rays. For this reason, PMMA has been used as a positive photo-resist material in lithography for electronic applications [2,3]. The propensity of degradation was attributable to a steric hindrance due to the methylester (CH_3OOC–) groups

[1] E-mail: leeeh@ornl.gov

0168-583X/99/$ – see front matter © 1999 Elsevier Science B.V. All rights reserved.
PII: S0168-583X(99)00129-9

attached to the PMMA backbone structure [4]. Large pendant groups restrict chain mobility and thus impede cross-linking. On the other hand, when PMMA was subjected to high energy ions such as 2 MeV Ar-ions, the surface hardness of PMMA increased dramatically, as a result of massive cross-linking, from the pristine value of 0.5 GPa to over 10 GPa after irradiation to a fluence of 1×10^{19} m^{-2} [1].

There has been a considerable discrepancy in regard to the interpretation of the mechanisms of scission and cross-linking for irradiated PMMA. In general, PMMA is regarded as a scissioning type polymer. However, Hall et al. [5] studied solubility changes as a function of fluence for PMMA irradiated with 20 keV electrons (2), 1.5 MeV H^+ (20), He^+ (200), and O^+ (800) ions; the numbers in the parenthesis are approximate initial LET values in eV/nm. LET is a measure of energy deposited per unit ion path length, often expressed in SI units of eV/nm/ion or simply eV/nm. They found that initially the solubility of PMMA increased progressively with increasing fluence, but subsequently decreased with further increase of fluence beyond a certain threshold value. Analysis indicated that the transition from soluble to insoluble occurred at lower fluence with increasing LET [6]. Moreover, for 20 keV e-beam irradiation, gelation did not occur up to a fluence of 6.25×10^{24} e/m^2 [7]. Mladenov and Emmoth [8] determined the minimum ion doses for complete dissolution of PMMA after irradiation with H^+, He^+, and Ar^+ ions of keV and MeV energies, and they correlated the increase of solubility (or scission) with electronic LET. On the other hand, Fink et al. [9] studied the structure of PMMA irradiated with various keV and GeV ion species. They attributed the formation of insoluble cyclic or polycyclic compounds (cross-linking) to electronic LET, contrary to the former conclusion. There has been considerable debate regarding the mechanisms for optical densification in the bombarded polymers: whether they are due to electronic or nuclear processes. Fink et al. ascribed the darkening of Kapton to the clusters of carbon atoms released from the macromolecules by direct knock-ons through the nuclear collision process [10]. On the other hand, Davenas et al. concluded that the optical density increase occurred predominantly by electronic processes [11].

In the past, many investigators studied PMMA because its non-gelling nature at low dose irradiation allowed them to study the mechanisms of scission and cross-linking [12]. Fig. 1 summarizes the scission yields of PMMA, G_s values, as a function of LET, which are extracted from various reports [12–29]. The G_s value is a quantitative measure of the specific chemical yield (here scission) per 100 eV of radiation energy absorption. In spite of the scatter, the G_s values showed fairly constant values, on average ~1.3, below a certain threshold LET value (~15 eV/nm), particularly when comparing the data from the same authors.

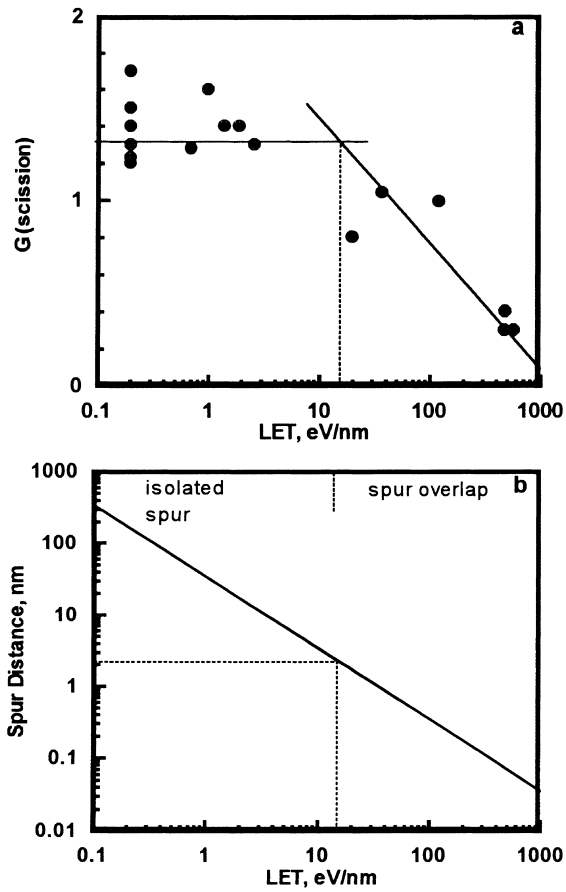

Fig. 1. Scission G_s values for PMMA irradiated with various irradiation sources (a) and calculated spur distances (b) as a function of LET.

The G_s values decreased with increasing LET beyond the threshold LET value, suggesting that a transition from scission to cross-linking occurs with increasing LET. In this paper, this peculiar LET dependence of G_s values is explained by exploring the track formation mechanisms.

This paper addresses fundamental processes involved with nuclear and electronic processes induced by ions, and clarifies the confusing issues in interpreting the ion-beam induced property changes such as the fluence dependent solubility of PMMA, the LET dependent G_s-values, and optical density changes of Kapton. Specifically, what are the roles of electronic and nuclear stopping and how do they affect materials' properties? Does electronic (or nuclear) stopping cause crosslinking or scission, or both? What are the differences between ionizing radiation such as e-beam and γ-rays and high energy ion-beams (HEIB) in the several hundred keV and several MeV ranges? What are the mechanisms involved in cross-linking and scission? These questions are answered by elucidating fundamental energy loss mechanisms involved with irradiation.

2. Nuclear and electronic stopping

When an energetic particle penetrates into a polymer medium, it loses energy by two main processes, namely, by interacting with target nuclei (screened) and by interacting with target electrons. The former process is called *nuclear stopping* and the latter *electronic stopping*.

Nuclear energy loss arises from collisions between the energetic particle and target nuclei, which cause atomic displacements and phonons. Nuclear energy loss by inelastic collision (nuclear reactions) is not considered here. Displacement occurs when the colliding particle imparts an energy greater than a certain displacement threshold energy, E_d, to a target atom. Otherwise, knock-on atoms cannot escape their sites and their energy dissipates as atomic vibrations (i.e., phonons). E_d is the energy that a recoil requires to overcome the binding forces and to move more than one atomic spacing away from its original site. Since the nuclear collision occurs between two atoms with electrons around protons and neutrons, the interaction of an ion with a target nucleus is treated as the scattering of two screened particles. Nuclear stopping is derived with consideration of the momentum transfer from ion to target atom and the interatomic potential between two atoms. Thus nuclear stopping varies with ion velocity as well as the charges of two colliding atoms. Nuclear stopping becomes important when an ion slows down to approximately the Bohr velocity (orbital electron velocity). For this reason, the maximum nuclear energy loss occurs near the end of the ion track. for high energy ions. The Bohr velocity can be derived from the uncertainty principle as $V_B \approx (1/4\pi\varepsilon_o)(e^2/\hbar) \approx 2.2\times10^6$ m/s, where $1/4\pi\varepsilon_o = 9.0\times10^9$ Nm^2/C^2, ε_o is the permittivity constant, e is a unit charge, and $\hbar$ is Planck's constant divided by 2π. The velocity of a 1 MeV He ion is about 6.9×10^6 m/s.

Electronic stopping is determined mainly by the charge state of the ion and its velocity. When an ion passes through a medium, its orbital electrons are stripped off in varying degree depending upon the ion velocity (V_{ion}). The effective charge on a positive ion is given, in terms of ion velocity (V_{ion}) and Bohr (orbital electron) velocity (V_B), by Northcliffe [30] as

$$Z^*_{eff} = Z\left[1 - a\exp\left(-b\frac{V_{ion}}{V_B}Z^{-2/3}\right)\right], \quad (1)$$

where Z is the atomic number, and a and b are fitting constants. There have been scores of proposed empirical formulae such as $Z^*_{eff} = Z\times[1-\exp(-k\beta/Z^{2/3})]$, where $\beta = V_{ion}/c$ and c is the speed of light. Somewhat different values have been assigned for coefficient 'k' by various authors; 25 by Pierce and Blann [31] and 130 by Barkas [32], for example. All expressions give a similar trend. He-ions are almost completely stripped to an average charge of +2 at around 1 MeV or $\gtrsim$ 0.3 MeV per amu. The higher the Z, the higher the energy required to fully strip an atom.

Electronic energy loss arises from electromagnetic interaction between the positively charged ion and the target electrons. One mechanism is called *glancing collision* (inelastic scattering, distant resonant collisions with small momentum

transfer) and the other is called *knock-on collision* (elastic scattering, close collisions with large momentum transfer). Both glancing and knock-on collisions transfer energy in two ways: electronic excitation and ionization. All excited electrons (plasmons) eventually lose energy as they thermalize. Electronic excitation is the process in which an orbital electron is raised to a higher energy level, whereas, in ionization, an orbital electron is ejected from the atom. Glancing collisions are quite frequent but each collision involves a small energy loss (<100 eV). On the other hand, knock-collisions are very infrequent but each collision imparts a large energy to a target electron (>100 eV). These knock-on electrons are often called δ-rays or secondary electrons. Theoretical and experimental evidence suggested that approximately one half of the electronic energy loss is due to glancing collisions and the other half to knock-on collisions [33, 34]. This phenomena is often referred to as the *equipartition principle* and has been confirmed by experiment [35], where two well defined peaks at low and high energy were observed for protons channeled through monocrystalline copper. The energy loss ratio for channeled and unchanneled protons was approximately 0.5. The 'best-channeled' particles had a stopping power of the order of one-half the stopping power in the corresponding solid. The half of the energy loss in the channeled direction was attributed to glancing collisions.

Nuclear collisions create recoil atoms and these recoil atoms also lose their energy through nuclear and electronic processes until all excited electrons and atoms are thermalized by dissipating energy through phonons and plasmons. For most ion energy ranges of interest, nuclear stopping by small atoms such as H or He is negligible because the Rutherford cross-section and momentum transfer by the low mass atoms is small. Nuclear stopping, however, becomes important for ion species with a large number of nucleons.

Fig. 2 summarizes the energy partitioning in the Monte Carlo simulation program *Stopping and Range of Ions in Matter* (SRIM) [36]. An example of average energy partitioning per ion for 100 keV Ar ions into polypropylene, calculated with the Kinchin–Pease approximation (described below)

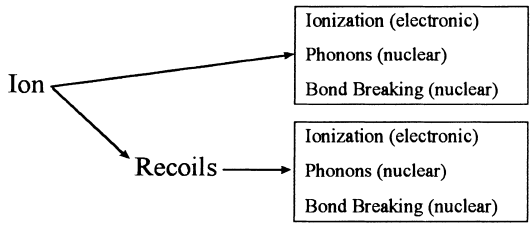

$$\textbf{Electronic LET} = (LET)^{ionization}_{by\ ion} + (LET)^{ionization}_{by\ recoils}$$

$$\textbf{Nuclear LET} = (LET)^{bonds}_{by\ ion} + (LET)^{bonds}_{by\ recoils} + (LET)^{phonons}_{by\ ion} + (LET)^{phonons}_{by\ recoils}$$

Fig. 2. Energy partitioning in SRIM. Here, since the bond breaking energy is equal to the number of vacancies times E_b, this energy is designated as LET(vacancies) in Fig. 3.

using the SRIM v. 96, is shown in Fig. 3. The electronic energy loss constitutes the ionization and excitation energy loss by the primary ion as well as by recoil atoms. Every recoiling target atom loses E_b (binding energy) when it leaves its site. E_b is the difference in energy for the atom in its site and removed to an infinite distance. Binding energy for most organic polymers is not known well. Typical lattice binding energies, E_b, of 1–3 eV, are suggested for organic compounds in the SRIM instruction manual. Nevertheless, actual binding energies could be higher considering strong covalent bonds in organic polymers. A usage of a different value of E_b affects the energy partition between bond breaking energy and phonon energy, but the total nuclear LET remains the same in SRIM calculation. In the SRIM calculation, the bond breaking energy (called the vacancy LET, because the number of vacancies which are produced by bond breaking are counted) is treated separately and is derived by multiplying the number of displacements (vacancies plus replacements) by E_b. In the Kinchin–Pease approximation described below, replacements are not calculated and so the displacement number is equal to vacancy number. The minimum or threshold energy required to break the bonds and displace the atom over a lattice potential is called the displacement energy (E_d). Although the values of E_d are not well known for polymers, they are believed to be in the range of 10–30 eV, considering the energy required in breaking strong covalent bonds and placing the

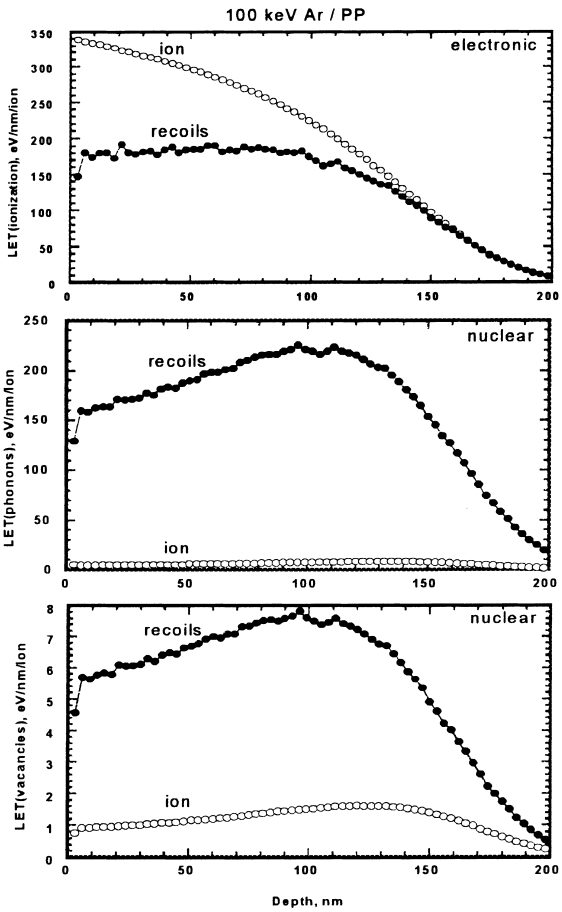

Fig. 3. SRIM calculated electronic (ionization) and nuclear (phonons and vacancy) energy losses for 100 keV Ar in polypropylene. For calculations, the values of 2 eV and 20 eV were used for the binding energy, E_b, and displacement energy, E_d, respectively.

released atom over a certain distance. Note that at least two bonds should be broken to release a carbon atom. When a recoil atom does not have sufficient energy to displace another atom, the remaining energy is dissipated in lattice vibration (phonons). The nuclear energy loss is equal to the sum of the phonon LET and vacancy LET (number of vacancies times E_b). The integrated area under the six curves sums to 100 keV, the energy received by the system. The phonon contribution from the ions is small compared with that of the recoils because one ion produces many recoils.

In the Kinchin–Pease approximation, the recoils are not individually followed in the Monte Carlo calculation. However, the flight paths of the primary ions are tracked and the energy losses are calculated using ZBL stopping powers [36] S_n and S_e formulas given below. The defect producing energy or damage energy (E_v) is obtained from the energy transferred (T) from the primary ion to a target atom by taking into consideration electronic losses which arise due to the interaction between overlapping electron shells during nuclear collisions. The electronic losses of the recoils are calculated using an approximation to the LSS theory developed by Norgett et al. [37]. The transferred energy and the damage energy are given below. The electronic (ionization and excitation) energy loss by recoils (E_r^I) is obtained by subtracting E_v from T.

$$T = \frac{4M_1M_2}{(M_1+M_2)^2} E \sin^2\left(\frac{\theta}{2}\right), \tag{2}$$

$$E_v = \frac{T}{1 + k_d g(\varepsilon_d)}, \tag{3}$$

$$E_r^I = T - E_v, \tag{4}$$

where E is the kinetic energy of the incident atom, θ is the scattering angle in the center of mass system, M_1 and M_2 are the mass numbers of the colliding and target atoms, respectively. The latter three parameters, which account for the electronic loss, are given by

$$k_d = 0.1337 Z_2^{2/3} M_2^{-1/2}, \tag{5}$$

$$g(\varepsilon_d) = \varepsilon_d + 0.40244\varepsilon_d^{3/4} + 3.4008\varepsilon_d^{1/6}, \tag{6}$$

$$\varepsilon_d = 0.01014 Z_2^{-7/3} T, \tag{7}$$

where Z_2 is the atomic number of the target atom. From the energy E_v, the number of displacements is calculated by employing a modified Kinchin–Pease model (NRT model [37]),

$$v_{NRT} = 0 \quad \text{if } E_v < E_d, \tag{8}$$

$$v_{NRT} = 1 \quad \text{if } E_d < E_v < 2.5E_d, \tag{9}$$

$$v_{NRT} = \frac{0.8E_v}{2E_d} \quad \text{if } E_v > 2.5E_d. \tag{10}$$

In the NRT model, the displacement efficiency factor 0.8 is introduced to account for realistic

atomic scattering instead of the hard core approximation where efficiency factor is unity (billiard ball type collision), and the number 2 in the denominator is included on the grounds that an atom must have a kinetic energy at least twice the displacement threshold energy in order to cause a net additional displacement. In the full SRIM calculation, total displacements include vacancies and replacement collisions.

As described already, both nuclear and electronic stopping depend upon the kinetic energy or velocity of the colliding atom because the velocity determines the interaction time. In the SRIM full cascade calculation, the ZBL stopping powers are used for both the primary ion and recoils. A mathematical expression for the nuclear stopping cross-section is given by

$$S_{\mathrm{n}} = \int_0^{\infty} T(E_0, p) 2\pi p \, \mathrm{d}p, \tag{11}$$

where E_0 is the initial kinetic energy of the atom, T the transferred energy defined above, and p is an impact parameter. p is the distance by which the collision misses being head-on, and is a measure of the directness of the collision or straightness of the flight path, which is determined by particle velocity and the interatomic potential between the two colliding particles.

A mathematical expression for the electronic stopping cross-section is given by

$$S_{\mathrm{e}} = \int I(v, \rho)(Z_1^* v)^2 \rho \, \mathrm{d}V, \tag{12}$$

where $I(v, \rho)$ is the stopping interaction function, v is the ion velocity, ρ is the target electron density, Z_1^* is the effective particle charge, and $\mathrm{d}V$ is a volume element. $I(v, \rho)$ varies with the particle velocity and plasma oscillation frequencies of the electrons in the stopping medium. Fast particles ($v \gg$ Bohr velocity) have little interaction time and so electronic stopping decreases with increasing velocity beyond this velocity. Slow particles ($v <$ Bohr velocity) pick up electrons, so have a lower effective charge. Therefore, a maximum in the electronic stopping occurs near the Bohr velocity. Linear energy transfer (LET) is simply given by

$$\frac{\mathrm{d}E}{\mathrm{d}x} = NS(E), \tag{13}$$

where N is the atomic density of target. In evaluating the damage produced by irradiation, the unit of displacements per atom (dpa) is often used. The expression of displacement dose in dpa is give by

$$\mathrm{dpa} = \frac{0.8}{2E_d}\left(\frac{\mathrm{d}E}{\mathrm{d}x}\right)_{\mathrm{nuclear}} \times \frac{\text{ion fluence}}{\text{target atomic density}}. \tag{14}$$

One dpa is the dose at which, on average, each atom has been displaced from its lattice position once. The term 'dose' is expressed often in terms of the energy deposited per unit mass of material, generally in units of eV/kg or Gy ($=100$ Rad), whereas the 'fluence' indicates the number of ions injected per unit area of target material (ions m^{-2}). In the conversion from fluence to dose, the SI unit of Gray (Gy) is obtained by multiplying the fluence (ions m^{-2}) by the LET (eV/nm) and dividing by the specific gravity of the target material (kg/m^3) and finally using a conversion factor of 1 Gy $= 6.24 \times 10^{18}$ eV/kg.

3. Ion tracks

Although a term 'short track' is often used to designate a continuous column of energy deposit (500–5000 eV) for a high-LET particle, here it simply means a passage of an ion. When a positively charged ion passes through a medium, orbital electrons in the stopping medium are pulled off by an electromagnetic force. These charge separations produce strong restoring forces. Consequently, oscillations of an electrostatic nature are set up, and the electron density, velocity, and electric field all oscillate with the plasma frequency ω_{p} [38]:

$$\omega_{\mathrm{p}} = \left[\frac{1}{4\pi\varepsilon_0}\frac{4\pi n e^2}{m_{\mathrm{e}}}\right]^{1/2}, \tag{15}$$

where e (C) and m_{e} (kg) are the charge and mass of the electron, n (m^{-3}) is the electron number density of the medium. An expression for the

radial extent of energy deposition, proposed by Chatterjee and Schafer [39], is given below in terms of this plasma oscillation frequency of the stopping medium as

$$r_c = \frac{\beta c}{\omega_p}, \tag{16}$$

where $\beta = V_{ion}/c$. r_c, called the physical core, is the range of fluctuation of electron density or energy for a period of plasma frequency pulse, or is the range of uncertainty in energy deposition at the epoch of initial energy deposition and can be derived from the uncertainty principle, $\Delta t \Delta E \approx \hbar$. r_c or Δr is given by $\Delta r \approx \hbar V_{ion}/\Delta E$ in consideration of $\Delta t \approx \Delta r / V_{ion}$. ΔE is an energy width over which an absorption can take place; later we define this energy as 'spur'. r_c varies with ion velocity and defines the range of energy deposition which occurs at a period of around 10^{-16} s, which is the earliest significant time and can be estimated from $\Delta t \Delta E \approx \hbar$ by taking $\Delta E \approx 20$ eV for a relativistic particle (0.99c or ~1000 MeV/nucleon). In this time scale, only electronic processes are possible since the time is too short for molecular motion. Molecular vibration becomes important at around 10^{-14} s, molecular motion and a local temperature rise occur at $\sim 10^{-13}$ s, diffusion processes start at $\sim 10^{-12}$ s [40].

The δ-rays also cause electronic excitation and ionization along the track, mostly outside the r_c. The maximum range of δ-rays can be calculated by the following relationship [41, 42]:

$$r_{max}\left[\frac{g}{cm^2}\right] = kW_{max}^{\alpha}, \tag{17}$$

where $k = 6 \times 10^{-6}$ g cm^{-2} (keV)$^{-\alpha}$, $\alpha = 1.097$ for $W_{max} < 1$ keV and $\alpha = 1.677$ for $W_{max} > 1$ keV. W_{max} is the maximum energy of δ-rays, which is derived from the kinematics consideration for head on collision between ion and electrons in the medium as

$$W_{max} = \frac{4 m_{ion} m_e}{(m_{ion} + m_e)^2} E_{ion}, \tag{18}$$

or as $W_{max} = 2 m_e v_{ion}/(1 - \beta^2)$ with the relativistic correction of mass for fast ions, where m_e is electron mass. A pictorial description of tracks is illustrated in Fig. 4 where the radial range of δ-rays is indicated by the radius, r_p, which is called the penumbra radius. Since a higher knock-on electron energy yields a smaller angle of ejection, r_p (radial) is always smaller than r_{max} (forward direction). r_p can be calculated by considering that the velocity and the energy of δ-rays in a radial direction are $v_\delta = v_{max} \cos\theta$ and $W \approx W_{max} \cos^2\theta$ and that the maximum momentum transferable to electrons in a radial direction occurs at the scattering angle of 45° (π/4). Hence, for $\alpha = 1, r_p \approx r_{max}/(2\sqrt{2})$ can be derived using $r_\delta \approx kW$ and $W \approx W_{max}\cos^2(\pi/4)$ and considering $r_p \approx r_\delta \sin(\pi/4) \approx kW \sin(\pi/4) \approx kW_{max}\cos^2(\pi/4) \sin(\pi/4) = r_{max}\cos^2(\pi/4)\sin(\pi/4)$.

The *initial* average energy densities within the core r_c, and core between r_c and r_p are given by Chatterjee and Schafer [43,44] below. The energy density within the core is mostly from glancing collisions and a small fraction of low energy knock-on electrons which are trapped inside the core (second term in the first equation below). r is the radial distance from the particle trajectory.

$$\rho_{core} = \left(\frac{LET}{2}\right) \Big/ [\pi r_c^2]_{gl} + \left(\frac{LET}{2}\right) \Big/ \left[2\pi r_c^2 \ln\left(\frac{e^{1/2} r_p}{r_c}\right)\right]_\delta, \quad r \leqslant r_c \tag{19}$$

$$\rho_{pen}(r) = \left(\frac{LET}{2}\right) \Big/ \left[2\pi r_c^2 \ln\left(\frac{e^{1/2} r_p}{r_c}\right)\right]_\delta, \quad r_c \leqslant r \leqslant r_p, \tag{20}$$

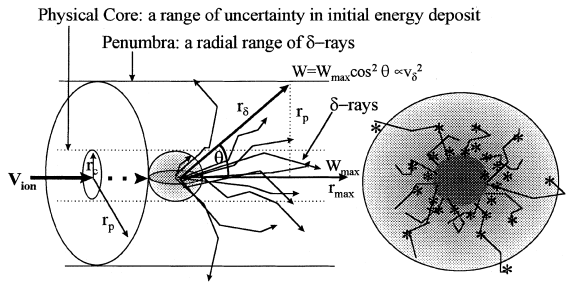

Fig. 4. Artist's rendition of ion track which shows physical core, r_c, penumbra, r_p, and δ-rays. W and r are the kinetic energy and the range of δ-rays.

$$\left[\frac{\mathrm{LET}}{2}\right]_{\mathrm{gl}} = [\pi r_{\mathrm{c}}^2]\left(\frac{\mathrm{LET}}{2}\right)\Big/[\pi r_{\mathrm{c}}^2]_{\mathrm{gl}}, \tag{21}$$

$$\left[\frac{\mathrm{LET}}{2}\right]_{\delta} = [\pi r_{\mathrm{c}}^2]\left(\frac{\mathrm{LET}}{2}\right)\Big/\left[2\pi r_{\mathrm{c}}^2 \ln\left(\frac{e^{1/2} r_{\mathrm{p}}}{r_{\mathrm{c}}}\right)\right]_{\delta} + \int_{r_{\mathrm{c}}}^{r_{\mathrm{p}}} \rho_{\mathrm{pen}}(r)\,\mathrm{d}(\pi r^2). \tag{22}$$

The energy density between r_c and r_p is from δ-rays. The equipartitioning of LET to glancing and knock-on collisions can be confirmed by converting the energy density to LET as shown in the third and fourth equations above. Values of r_c and r_p vary with the specific energy of the particle (energy per nucleon) as mentioned already.

The ion path is thus described by a cylindrical trajectory defined by the physical core with radius r_c (the approximate limiting distance from the particle trajectory at which an electronic excitation occurs initially), and the penumbra with radius r_p (the outermost cylindrical boundary of the δ-rays or secondary electrons) [44]. Another radius used in this model is the radius of the chemical core which lies between the physical core (r_c) and penumbra (r_p). The chemical radius defines a range where chemical reactions occur. The chemical radius (r_{ch}) is thus determined by the diffusion and reaction rates of active chemical species such as radicals, cations, anions, electrons, and other activated chemical species. Shapes and sizes of track entities are first defined and then followed by the formation of active chemical species, diffusion, and their interaction via chemical and coulombic forces. Some chemical species recombine and neutralize in a dense chemical sea, some diffuse out to the penumbra and mingle together with chemical species induced by δ-ray, establishing a fairly large effective radius. Since the chemical radius is difficult to measure or calculate in reality, here, we use a term 'effective' radius instead, which defines the extent to which the energy density or radical concentration is significant for a given process. Cross-linking, scission, and other chemical reactions occur within this effective radius. Most cross-linking and other chemical reactions occur near r_c where concentrations of radicals and ion pairs are high because of the slow migration of radicals in a viscous medium. In particular, for low LET tracks, δ-rays develop independently and have very little effect on crosslinking. With increasing LET, energy density increases, and so does the effective radius. However, one should be cautioned that, although low Z ions such as H^+ may have large r_c and r_p at high energy (note that r_c and r_p are only ion velocity dependent parameter), the effective radius is small because of low charge state or low LET. This point is examined further below by appealing to the concept of 'spur' and its relation to LET.

4. Spurs

The stopping power formula or the concept of LET is implicitly based on the continuous slowing-down approximation. In reality, energy deposition occurs discretely, not continuously. This is because electronic excitation is restricted by quantized energy levels and ionization is restricted by a certain potential energy barrier which has to be overcome for electrons to be released from the orbit. In addition, atomic displacement requires a certain threshold energy to break the bonds and move the atom over a certain potential barrier due to surrounding atoms. In most cases, a creation of an ion pair involves a removal of two or more electrons, for example, one electron from a hydrogen atom and one or more from a carbon atom. Ionization potentials for the first, second, and third electrons of carbon atom are 11.26, 24.38 and 47.89 eV, respectively. Ionization of carbon atom to C^{3+} thus requires at least 83.53 eV. This discrete energy loss entity is often called a 'spur'. Most of the energy loss for ionization events or spur energy lies within 100 eV, with an average value of 30–40 eV for polymers [40, 45], which is approximately equal to the average energy required to produce one ion or radical pair. Of course, some of the energy is used for excitation, so the spur energy is larger than the sum of the ionization energy needed to create the ion pairs.

5. LET and spur distance

As mentioned above, energy transfer or loss occurs discretely as spurs along the ion track

instead of a continuous decay in energy. Thus changing the LET means changing the spur separation in the track or spur density. The distance between spurs can be calculated by dividing the spur energy by the LET. For example, for a spur energy of 40 eV and LET values of 2 eV/nm and 400 eV/nm, the spur distances are 20 nm and 0.1 nm, respectively. For low LET, spurs are widely separated and occur independently. With increasing LET, more radical pairs are created within the track radius, spurs are connected or overlapped, high radical concentration gradient is established, and so the effective radius increases. An effective radius for cross-linking can be estimated in terms of spur density by imposing a condition that at least one radical pair (or spur) is required per nm^3, since the distances between two polymer chains are in the nm range for most polymers and two radicals must be in neighboring chains for cross-linking to occur, (e.g., $LET/\pi r_{eff}^2 = 40$ eV/nm^3 for a spur energy of 40 eV). Of course, this approach grossly overestimates the radius because a significant fraction of radicals do not contribute to cross-linking due to recombination. In fact, several thousands of spurs were required per nm^3 to achieve a saturation hardness in He and Ar ion irradiated polystyrene [46], suggesting that most radicals were neutralized. It does, however, provide a qualitative means to appraise experimental data. On the other hand, the effective radii may be larger than those defined by the one spur per /nm^3 assumption for fluid systems where radicals and other chemical species can readily diffuse.

6. Electronic vs nuclear LET

An important question is what controls the magnitude of cross-linking and scission. During irradiation, various physical and chemical processes take place in the polymer. Nuclear collisions cause atomic displacements, which can then lead to chain scission or release of pendant atoms. Superposition of phonon waves can also lead to bond breakage, but the probability of such events is small because phonons have insufficient energy density to start with. Polymers have a fairly large free volume, often larger than 20%, and atomic density in such a loose system is relatively small compared to that in a medium with a compact lattice structure, such as a metal. Therefore, in polymers, most nuclear displacements occur fairly independently. The probability to cause simultaneous displacement of two atoms from neighboring chains and create two radical pairs for cross-linking is small in nuclear processes. Heavy and low energy ions with less than a few keV have large nuclear LET and are thus generally not desirable for cross-linking. An excellent example for the nuclear displacement damage effect was demonstrated by Hunn and Christensen [47]. They were able to lift free-standing, single crystal diamond layers by causing a maximum damage ~2 μm depth below the crystalline diamond surface with 4–5 MeV C-ions and selectively oxidizing the damaged layer. An amorphized layer underlying a crystalline diamond surface was also confirmed by Rutherford backscattering spectroscopy in a channeled geometry for 1 MeV Ar irradiated diamond, in that disordering was the least near the surface where the electronic LET was the highest [48]. An important implication of these results is that the displacement damage followed the nuclear LET profile and that the least damage was observed at the surface where the electronic LET was maximum.

On the other hand, when the electronic LET is high, a considerable volume around the ion projectile is influenced because of the coulombic field produced by glancing collisions and ionization (δ-rays) by knock-on collisions. This results in production of active chemical species, cations, anions, radicals, and electrons along the polymer chains. Coulombic attraction and repulsion among these active species cause violent bond stretching and segmental motion in the polymer chains, which can then lead to cross-linking as well as bond breakage. Thus, both electronic and nuclear energy transfer can induce crosslinking as well as scission. However, as pointed out above, nuclear stopping causes more scission due to the nature of independent displacement damage and the simultaneous production of two radicals in neighboring chains is low. On the other hand, electronic stopping cause more cross-linking due to collective excitation (plasmons), which produces a large

excited volume thereby resulting in coercive interaction among the ions and radical pairs produced within the volume. This trends have been confirmed by G-value and hardness measurements as well as other experiments [49,50]. With increasing ion energy, electronic LET increases and nuclear LET decreases. As shown in Fig. 5, electronic LET becomes an even more important factor for ions of 1 MeV compared to 100 keV. The magnitude of ionization varies with ion velocity and charge state. Thus it is desirable to use atomic species with large atomic number and employ high energy ions, so long as the velocity of the ion is not too high and so the energy density (LET) does not become too small due to small stopping power and large r_c and r_p. Not that too fast ion has a short interaction time and yields large r_c and r_p.

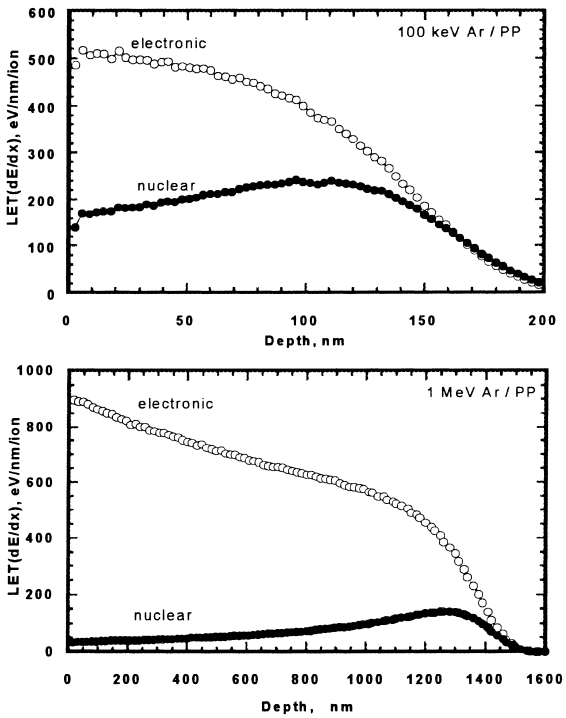

Fig. 5. SRIM calculated electronic (ionization) and nuclear (phonons + vacancies) LET for 100 keV and 1 MeV Ar ion irradiation of polypropylene. For calculations, the values of 2 eV and 20 eV were used for the binding energy, E_b, and displacement energy, E_d, respectively.

7. High vs low LET

As discussed already, the magnitude of ionization depends upon the deposited energy along the ion track or LET. The electronic LET for 1 MeV Ar is about 960 eV/nm for polystyrene, whereas those of e-beam and γ-rays are in the range of 0.2–0.36 eV/nm. Increasing the energy of e-beam or γ-rays does not increase the LET due to the limited effective charge or ionizing capacity; only the depth of penetration increases with increasing energy beyond a certain energy. For 1 MeV Ar ions, about 24 (960/40) ion pairs or spurs are created per nm, whereas, for e-beam or γ-rays, only 0.009 (0.36/40) spurs are created per nm. In other words, the average distance between the spurs is 0.042 nm (40 eV/ 960 eV/nm) for 1 MeV Ar and 111 nm (40 eV/0.36 eV/nm) for e-beam or γ-rays. In the case of high LET, spurs overlap, the probability for two radical pairs to be in neighboring chains is increased, and cross-linking is facilitated. For low LET, spurs develop far apart and independently, the deposited energy tends to be confined in one chain (not in the neighboring chain) leading to scission. For this reason, low LET e-beams are used in photolithography to make PMMA soluble. However, it should be pointed out that cross-linking is also polymer structure dependent, and even low LET ionizing radiation sources such as e-beam and uv can cause a limited degree of cross-linking for certain polymers.

8. LET dependence of G_s values

Assuming an average spur energy of 35 eV, one can calculate the spur distances for PMMA irradiated by the various irradiation sources shown in Fig. 1(a). Average distances between spurs are calculated by dividing 35 eV by the LET (eV/nm) values. The calculated spur distances are plotted as a function of LET in Fig. 1(b). The spur distance decreases with increasing LET and thus the probability of spur overlap increases with increasing LET. In Fig. 1(a), the data indicated that scission was dominant for LET values less than 15 eV/nm, implying that spurs were isolated below this LET range. Scission yield decreased with

increasing LET, shifting the regime from scission to cross-linking progressively. From Fig. 1(b), it can be seen that the spur distance is about 2 nm for an LET value of 15 eV/nm. This suggests that cross-linking becomes facile when the spur distance approaches 2 nm, which is approximately the intermolecular chain distance in polymers. This result is seemingly in accord with the condition that cross-linking can occur only when two dangling radical pairs are in neighboring chains.

9. Ion-beam induced property changes

Various gaseous molecular species are released during irradiation. The most prominent emission is hydrogen, followed by less abundant heavier molecular species which are scission products from the pendant side groups and chain-end segments, and their reaction products. Figure 6 illustrates various functional chemical entities created by irradiation. Crosslinking occurs when two free dangling ion or radical pairs on neighboring chains unite, whereas double or triple bonds are formed if two neighboring radicals in the same chain unite. It has been well established that mechanical, physical, and chemical property changes in polymers are determined by the magnitude of crosslinking and scission, and that crosslinking enhances mechanical stability while scission degrades mechanical strength [51]. Property changes induced by ion-beam irradiation and potential application areas were described in detail in references [1] and [52]. The main features are summarized below.

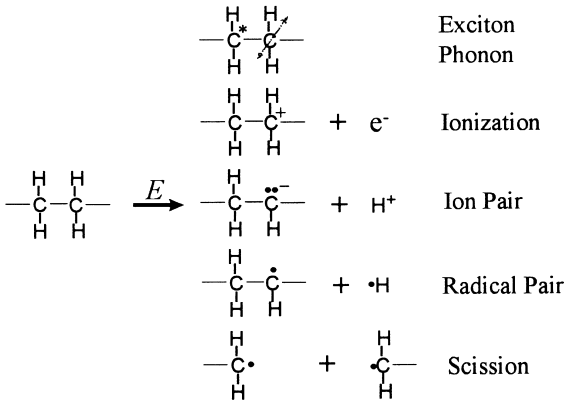

Fig. 6. Typical consequences induced by ion irradiation which include electronic excitation, phonons, ionization, ion pair formation, radical formation, and chain scission.

Cross-linking generally increases hardness and slows diffusion, improves wear and scratch resistance, and decreases solubility in chemical solvents. Electrical conductivity and optical density increase due to the formation of cross-links and conjugated double and triple bonds by irradiation. The delocalized π-electrons in the conjugated bonds are loosely bound and thus more mobile than the covalent σ-bond electrons. Furthermore, charge carrier mobility increases by cross-links which facilitate the transport of charge carriers across the chains. Otherwise, charge carriers must hop across the chains for conduction. The loosely bound π-electrons can be excited by the energies of visible light, and thus color changes occur because light is absorbed when these electrons are excited. Radiation induced defects such as anions and radicals (donors) and cations (acceptors) form a broadened band in the band gap and result in the absorption of light as well. Energetic blue light is absorbed first and the color changes from pale yellow to reddish brown and eventually to a dark color with increasing irradiation dose. At very high doses, a metallic luster appears because light is scattered by the abundant π-electrons similar to the effect of free electrons in metals. On the other hand, scission causes bond breakage and increases disolution of polymers in solvents. This feature has been used for lithography with positive-resists in the electronic industry [5].

10. Conclusions

Interaction mechanisms of charged particles with polymeric materials were discussed in view of nuclear and electronic stopping. While dominant processes caused by nuclear stopping are atomic displacements, electronic processes induce collective excitation of atoms and produce δ-rays. It was elucidated that electronic processes enhance cross-linking whereas nuclear processes enhance scission. Cross-linking and scission mechanisms were

explained by employing the concepts of LET, ion track, and spur. High LET tracks have a large effective radius and spurs overlap more compactly facilitating cross-linking, whereas, in low LET tracks, spurs develop independently, often leading to scission. Since electronic LET depends upon the ion velocity and its achievable charge state or proton number, high LET can be achieved by using ion species with high atomic number and by increasing ion energy. Electronic LET dictates cross-linking whereas nuclear LET dictates scission, but each has its own merits and applications: improvement of hardness and scratch resistance by cross-linking vs increase of solubility by scission, for example. Ion-beam induced property changes were briefly reviewed. The fundamental principles and the application examples presented in this paper can serve as a guidance in processing materials for industrial applications.

Acknowledgements

This research was sponsored by the Division of Materials Sciences, US Department of Energy, under contract No. DE-AC05-96OR22464 with Lockheed Martin Energy Research Corporation. The author wishes to thank Drs. M.B. Lewis, R.E. Stoller, and J. D. Hunn for invaluable discussions and for reviewing this manuscript.

References

[1] E.H. Lee, G.R. Rao, L.K. Mansur, TRIP 4 (1996) 229.
[2] J.N. Randall, D.C. Flanders, N.P. Economou, J.P. Donnelly, E.I. Bromley, Appl. Phys. Lett. 42 (1983) 457.
[3] T.M. Hall, A. Wagner, L.F. Thompson, Appl. Phys. Lett. 53 (1982) 3997.
[4] A. Chapiro, Radiation Chemistry of Polymeric Systems, Wiley, New York, 1962, p. 352.
[5] T.M. Hall, A. Wagner, L.F. Thompson, J. Appl. Phys. 53 (1982) 3997.
[6] E.H. Lee, G.R. Rao, L.K. Mansur, in Radiat. Phys. Chem., unpublished.
[7] K. Hashimoto, T. Koizumi, T. Sajashita, K. Kawakita, N. Nomura, Nucl. Instrum. Meth. Phys. Res. B 39 (1989) 813.
[8] G.M. Mladenov, B. Emmoth, Appl. Phys. Lett. 38 (1981) 1000.
[9] D. Fink, L.T. Chadderton, F. Hosoi, H. Omichi, T. Sasuga, L. Wang, R. Klett, J. Hillenbrand, A. Schmoldt, Nucl. Instr. Meth. Phys. Res. B 91 (1994) 146.
[10] D. Fink, M. Muller, T. Lewis, P. Chadderton, H. Cannington, R.G. Elliman, D.C. McDonald, Nucl. Instr. Meth. Phys. Res. B 32 (1988) 125.
[11] J. Devenas, G. Boiteux, M. Fallavierm, Nucle. Instr. Meth. Phy. Res. B 38 (1989) 796.
[12] M. Dole, The Radiation Chemistry of Macromolecules, Academic Press, New York, 1973, p. 103.
[13] B.W. Yates, D.M. Shinozaki, J. Polym. Sci. 31 (1993) 1779.
[14] C.U. Pittman Jr., C.Y. Chen, M. Ueda, J.N. Helbert, J.H. Kwiatkowski, J. Polym. Sci. Polym. Chem. 18 (1980) 3413.
[15] L.A. Wall, D.W. Brown, J. Phys. Chem. 61 (1957) 129.
[16] J.N. Helbert, C.Y. Chen, U. Pittman Jr., G.L. Hagnauer, Macromolecules 11 (1978) 1104.
[17] W. Schnabel, H. Sotobayashi, Polym. J. 8 (1976) 423.
[18] J.H. Lai, J.H. Herbert, Macromolecules 11 (1978) 617.
[19] W. Burlant, D. Green, C. Taylor, J. Appl. Polym. Sci. 1 (1959) 296.
[20] T. Bowmer, E. Reichmanis, C.W. Wilkins Jr., M.Y. Hellman, J. Polym. Sci., Polym. Chem. (1982) 2661.
[21] T.M. Hall, A. Wagner, L.F. Thompson, J. Appl. Phys. 53 (1982) 3997.
[22] H. Saeki, J. Electrochem. Soc. 134 (1987) 1194.
[23] A.R. Shiltz, P.I. Roth, G.B. Rathmann, J. Polym. Sci. 22 (1956) 495.
[24] S. Egusa, K. Ishigure, Y. Tabata, Macromolecules 12 (1979) 939.
[25] H. Kudoh, T. Sasuga, T. Seguchi, Proceedings 7th Int. Symp. On Advanced Nuclear Energy Research, Recent progress in accelerator beam applications, March 18–19, 1996 Takasaki, Japan, JAERI-Conf. 97-003, p. 273.
[26] H. Kudoh, T. Sasuga, T. Seguchi, Polymer 14 (1996) 2903.
[27] H. Kudoh, T. Sasuga, T. Seguchi, Radiat. Phys. Chem. 50 (1997) 299.
[28] W. Schnabel, S. Klaumünzer, H. Sotobayashi, Y. Tabata, F. Asmussen, Macromolecules 17 (1984) 2108.
[29] S. Egusa, K. Ishigure, Y. Tabata, Macromolecules 12 (1979) 939.
[30] L.C. Northcliffe, Phys. Rev. 120 (1960) 1744.
[31] E. Pierce, M. Blann, Phys. Rev. 173 (1968) 990.
[32] H. Barkas, Nuclear Research Emulsions, vol. 1, Chap. 9, Academic Press, New York, 1963, p. 371.
[33] A. Chatterjee, H.D. Maccabee, C.A. Tobias, Radiat. Res. 54 (1973) 479.
[34] L.C. Feldman, J.W. Mayer, S.T. Picraux, Materials analysis by ion channeling, ch. 2, Academic Press, New York, 1982.
[35] M. Kaminsky, Bull. Amer. Phys. Soc. 12 (1967) 635.
[36] J.F. Ziegler, J.P Biersack, and U. Littmark, The Stopping and Range of Ions in Solids, vol. 1, Pergamon Press, 1985, the program is down loadable from the world wide web at www.research.ibm.com.
[37] M.J. Norgett, M.T. Robinson, I.M. Torrens, Nucl. Eng. Design 33 (1975) 50.

[38] J.D. Jackson, Classical Electrodynamics, 2nd ed., Wiley, New York, 1975, p. 492.
[39] A. Chatterjee, H.J. Schafer, Radiat. Environ. Biophys. 13 (1973) 479.
[40] J.L. Magee, A. Chatterjee, Chapter 1, 5, and 6 in Radiation Chemistry, in: Farhataziz and M.A.J. Rodgers (Eds.), Principles and Applications, VCH Publishers, New York, 1987.
[41] J.J. Butts, R. Katz, Radiation research 30 (1967) 855.
[42] M.P.R. Waligorski, R.N. Hamm, R. Katz, Nucl. Tracks Radiat. Meas. 11 (1986) 309.
[43] J.L. Magee, A. Chatterjee, J. Phys. Chem. 84 (1980) 3529.
[44] J.L. Magee, A. Chatterjee, Chapter 4, in: G.R. Freeman, (Eds.), Kinetics of nonhomogeneous processes, Wiley, New York, 1987.
[45] G.D. Zeiss, W.J. Meath, J.C.F. MacDonald, D.J. Dawson, Radiat. Res. 63 (1975) 64.
[46] E.H. Lee, G.R. Rao, L.K. Mansur, Materials Science Forum 248/249 (1996) 135.
[47] J.D. Hunn, C.P. Christensen, Solid State Technol. 37 (1994) 57.
[48] W.R. Allen, E.H. Lee, Mat Res. Soc. Symp. Proc. 279 (1993) 333.
[49] E.H. Lee, G.R. Rao, M.B. Lewis, L.K. Mansur, J. Mater. Res. 9 (1994) 1043.
[50] M.B. Lewis, E.H. Lee, G.R. Rao, J. Nucl. Mater. 211 (1994) 46.
[51] J.M. Cowie, Polymers: Chemistry & Physics of Modern Materials, Intertext Books, Billings, Worcester, Great Britain, 1973 p. 283.
[52] E.H. Lee, Chapter 17 in Polyimides, in: K. Mittal, M. Ghosh (Eds.), Fundamental Aspects and Technological Applications, Marcel Dekker, 1996, pp. 471–503.